JPP Journal of Pharmacy and Pharmacology

ROYAL PHARMACEUTICAL SOCIETY

JPP Journal of Pharmacy and Pharmacology

JPP 2011, 63: 333–341

Received May 17, 2010
Accepted November 3, 2010
DOI
10.1111/j.2042-7158.2010.01228.x
ISSN 0022-3573

Research Paper

Advancing in-vitro drug precipitation testing: new process monitoring tools and a kinetic nucleation and growth model

Yvonne E. Arnold[a,b], Georgios Imanidis[a,b] and Martin T. Kuentz[a]

[a]Institute of Pharma Technology, University of Applied Sciences Northwestern Switzerland, Muttenz and [b]Division of Pharmaceutical Technology, University of Basel, Basel, Switzerland

Abstract

Objectives Poorly soluble weak bases often precipitate during intestinal passage, potentially leading to incomplete drug absorption. The underlying in-vivo and in-vitro drug precipitation mechanisms are not well understood. Thus, new analytical tools and a kinetic nucleation and growth model were introduced to in-vitro drug precipitation testing in biorelevant media.

Methods A drug precipitation test was used to simulate the transfer from the stomach to the intestine. Changes in the acceptor vessel were monitored using online dynamic image analysis and inline Raman spectroscopy. The concentration profiles of the model drug dipyridamole were analysed by high-performance liquid chromatography and the resulting data were fitted with a set of differential equations.

Key findings The dynamic image analysis revealed a complex structure of the precipitated dipyridamole particles, which were described as star-like crystals or aggregates of elongated primary particles. Raman spectroscopy allowed the precipitation over time to be monitored. Using the kinetic nucleation and growth model to describe this process demonstrated perfect agreement with the experimental data.

Conclusions The analytical methods and the kinetic model provided new insights into biorelevant drug precipitation and could in the future support formulation development.

Keywords drug precipitation; dynamic image analysis; kinetic nucleation and growth model; Raman spectroscopy

Introduction

New drug candidates in pharmaceutical development are often poorly water-soluble compounds. This leads to challenges in selecting the right formulation principle that on the one hand brings the drug into solution and on the other hand also keeps it in the solubilised state during the entire gastrointestinal passage. The aqueous solubility is influenced by the physicochemical nature of the compound. Therefore, high lipophilicity or comparatively low lipophilicity in combination with a predominant hydrophobicity can result in poor solubility.

Moreover, drug ionisation plays an important role. If the pH is below the pK_a, the solubility of weak bases is high in comparison with pH values exceeding the pK_a.

Under physiological conditions, drugs move from an acidic environment in the stomach to a pH of about 6.5 in the upper intestine, rendering weak bases prone to precipitation under these conditions. This relevant pH change during the gastrointestinal passage is influenced by food, concomitant treatment with antacids and age.[1–4]

A biorelevant transfer test is a useful tool to simulate such precipitation processes *in vitro*. In the literature, different transfer tests were reported that describe pumping of the acidic medium containing solubilised drug into the neutral intestinal medium.[5–8] Besides this transfer, the composition of the medium is an important aspect. Biorelevant media consider drug solubilisation in mixed micelles and therefore better mimic the physiological situation than pure buffer solutions. However, the debate about best-suited medium composition is still ongoing.[9] The choice of technical parameters such as the paddle speed or the transfer pump rate has also been debated.[5] In particular, it is reasonable to vary the transfer pump rate since gastric emptying is also subject to variation.

Correspondence: Martin T. Kuentz, University of Applied Sciences Northwestern Switzerland, Institute of Pharma Technology, Gründenstr. 40, CH-4132 Muttenz, Switzerland. E-mail: martin.kuentz@fhnw.ch

Precipitation is a complex process involving two different mechanisms. It starts with nucleation from a supersaturated solution followed by growth of the resulting particles. Furthermore processes such as Ostwald ripening or aggregation can occur.[10,11] Such aspects of drug precipitation were studied earlier, but mainly in the framework of drug substance crystallisation in chemical synthesis.[12] Here, the LaMer diagram was used as a first approach to predict substance precipitation by focussing on the solubilised amount of drug.[13] In the meantime, the understanding of compound supersaturation has evolved and a review article recently focused on pharmaceutical systems.[14] The activation energy for nucleation, ΔG^*, was described as the driving force of the nucleation process. In the simple case of homogenous nucleation, assuming spherical clusters, it can be calculated using the following equation:[14]

$$\Delta G^* = \frac{16\pi \cdot V_M^2 \gamma_{ns}^3}{3(k_b T \ln(S))^2} \quad (1)$$

where V_M holds for the molecular volume of the precipitating compound and γ_{ns} is the interfacial energy per unit area between the cluster and the surrounding solvent. The equation further includes the Boltzmann's constant, k_b, and the degree of supersaturation, S. The latter parameter is simply the ratio of the solute concentration in the supersaturated state divided by the equilibrium solubility. This is an important equation for ΔG^*, which displays the key parameters for the nucleation process under ideal conditions. However, it must be noted that the presence of polymers or other colloids can change precipitation behaviour. Apart from the described ideal case, a heterogeneous precipitation has been described in the literature.[11] This increased level of complexity is one reason for the still limited understanding of the precipitation processes *in vivo*. Such lack of understanding exists also in the area of modern in-vitro precipitation testing. Recently, Sugano pioneered the use of a nucleation and growth model in biopharmaceutical testing.[15] However, the simulated concentrations could not adequately predict the experimental concentration–time profiles in all cases. As a consequence, there are still open questions with respect to parameters influencing the precipitation mechanisms, starting from the composition of the biorelevant media to the transfer rate of the simulated gastric fluid into the simulated intestinal fluid. Moreover, there is a need for novel analytical tools to monitor the morphology and number of precipitated particles, as well as for the study of subsequent processes such as aggregation.

The aim of the present study was to introduce new analytical tools for real-time monitoring in a biopharmaceutical transfer test. Drug precipitation was monitored by online dynamic image analysis and inline disperse Raman spectroscopy. Moreover, a power law modelling approach[16] was adapted for the first time to a biopharmaceutical transfer test. We proposed a kinetic nucleation and growth model that also considered the pump rate used in the test. Dipyridamole was selected as a model compound. It is a weakly basic Biopharmaceutical Classification System II drug, $pK_a = 6.4$,[17] which is known for its pH-dependent solubility.[4–6]

Materials and Methods

Materials

Dipyridamole, ammonium acetate, diethylamine, maleic acid, sodium chloride, sodium hydroxide and sodium oleate were purchased from Sigma-Aldrich (Buchs, Switzerland). Pepsin was obtained from Hänseler (Herisau, Switzerland), sodium taurocholate was purchased from Prodotti Chimici e Alimentari S.p.A. (Basaluzzo, Italy) and glycerol monooleate was supplied by Danisco (Copenhagen, Denmark). Phopsphatidylcholine was obtained from Lipoid (Ludwigshafen, Germany).

Fasted state simulated gastric fluid (FaSSGF) and fed state simulated intestinal fluid V2 (FeSSIF V2) were used as biorelevant media. They were prepared as previously reported using the compositions described in Table 1.[9]

In-vitro drug precipitation transfer test

The in-vitro transfer test was conducted using a US Pharmacopeia II apparatus (DT 600; ERWEKA, Heusenstamm, Germany) and dipyridamole was solubilised in 250 ml FaSSGF to reach a drug concentration of 3 mg/ml. This solution was pumped into 500 ml FeSSIF V2 at transfer rates of 4 and 9 ml/min using a peristaltic pump (Petro Gas Ausrüstungen, Berlin, Germany). The media were maintained at 37 ± 0.5°C and stirred with a paddle speed of 100 rev/min. Samples ($n = 3$) of 1 ml were taken at different time points, followed by filtration through a regenerated cellulose membrane with a pore size of 0.45 μm (SUN-SRi, Rockwood, TN, USA). The samples were then instantly diluted with 1 ml medium and visually checked so that no drug precipitation occurred in further analysis. Subsequently, the concentration of dissolved dipyridamole was determined by high-performance liquid chromatography (HPLC). The sample volume taken from the acceptor medium was replaced at each time point with fresh temperature-adjusted FeSSIF V2 medium and the entire transfer test was conducted over 3 h. Figure 1 depicts the biopharmaceutical transfer test together with the analytical monitoring tools.

HPLC assay

HPLC measurements were performed on a LiChrospher 60, RP select B 125-4 (5 μm) column (Merck, Darmstadt, Germany). The mobile phase consisted of 0.5% aqueous

Table 1 Composition of biorelevant media

	FaSSGF	FeSSIF V2
Sodium taurocholate (mM)	8×10^{-2}	10
Phosphatidylcholine (mM)	2×10^{-2}	2
Glycerol monooleate (mM)	–	5
Sodium oleate (mM)	–	0.8
Maleic acid (mM)	–	55.02
Sodium chloride (mM)	34.2	125.5
Sodium hydroxide (mM)	–	69.9
Pepsin (μM)	1.24	–
pH	1.6	5.8

FaSSGF, fasted state simulated gastric fluid; FeSSIF V2, fed state simulated intestinal fluid V2.

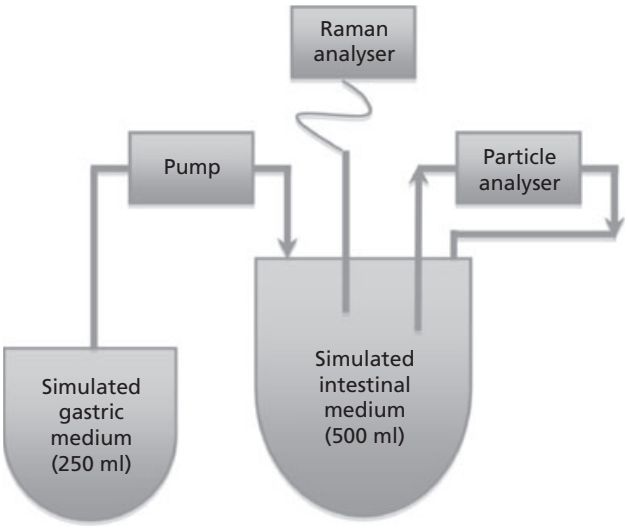

Figure 1 Schematic diagram of the transfer test including the inline Raman spectrometer and the dynamic image analysis system as particle analyser.

ammonium acetate solution, 0.2% methanolic diethylene amine solution and acetonitrile (30 : 55 : 15 v/v). Samples of 5 μl were injected and analysed at a flow rate of 1 ml/min and a detection wavelength of 294 nm.[18]

A new calibration line over the range 0.089–1.426 mg/ml was determined for each series of measurements. All calibration lines were over a linear concentration range and exhibited an R^2 of greater than 0.999. The limit of detection was 0.053 $\pm$ 0.000 mg/ml ($n = 4$) of dipyridamole concentration.

Dynamic image analysis

Online dynamic image analysis was performed on an XPT-C particle analyser (PS Prozesstechnik GmbH, Basel, Switzerland). Using a peristaltic pump (Ismatec SA, Glattbrugg, Switzerland), the acceptor medium was transported through a measuring cell equipped with a Flea 2, 1392 $\times$ 1032 pixel CCD camera to analyse the formation of particles/aggregates. The camera performed 70 measurements/min and the average is reported. Data on number, shape and size of the particles or aggregates were gathered. The number of particles was counted in a total volume of 153 mm^3 and subsequently used to calculate the corresponding particle concentrations. The particle sizes were evaluated as Waddle Disk Diameter (WDD), representing the diameter of a disk with an equal area to the projected area (A) of the observed particle/aggregate:

$$WDD = 2\sqrt{\frac{A}{\pi}} \qquad (2)$$

Raman spectroscopy

The in-vitro transfer test was monitored in the acceptor phase using a dispersive Raman spectrometer, RamanRXN1 Systems (Kaiser Optical Systems. Inc., Ann Arbor, MI, USA) equipped with a CCD camera and a fibre optic probe (spot size 0.007 mm^2). A diode laser emitting at 785 nm with a power of 400 mW was used. An exposure time of 20 s every 3 min was chosen to record a spectrum over the range of 100–3425 cm^{-1}, while averaging every spectrum over five scans. To avoid the influence of light on the measurements, the dissolution vessel was completely wrapped in aluminium foil.

Mathematical modelling and statistical analysis

We developed a mathematical model that was based on a power law for describing the kinetics of nuclei formation and growth.[16] This model took into account the transfer of simulated gastric to intestinal fluid at a set rate. The resulting equations were fitted to the experimental concentration data using EASY-FIT software (K. Schittkowski, University of Bayreuth, Germany). The algorithm of this program was minimising the sum of squared residuals. However, since it was not possible to estimate all parameters simultaneously, a two-step procedure was applied. Fitting was performed with fixed exponent values set over a range of 2 to 9 for the nucleation exponent and we tested values of 1 to 2 for the growth exponent in line with the reported literature span.[16] Each fitting with a given exponent provided residuals for calculating the root mean square error. This value was subsequently minimised using Statgraphics Centurion (Statpoint Technologies, Inc., Warrenton, VA, USA) to find the best exponent combination for each flow rate separately.

For the statistical treatment of the Raman data, all spectra were corrected for the baseline. A wavelength range from 504 to 2922 cm^{-1} was selected for a multivariate analysis of Raman intensities. Accordingly, the response of the model was the precipitated drug as obtained from the HPLC data. The calculations were performed using the software IC Quant Module 1.0 (Mettler Toledo, Greifensee, Switzerland) to propose an optimal partial least square model. This model exhibited on the one hand a minimal root mean square error of calibration, while on the other hand the predicted residual sum of squares was minimal.

Finally, the standard errors in the figures and tables were calculated using Microsoft Excel 2003.

Results

Solubility of the model drug dipyridamole

The measured equilibrium solubility of dipyridamole at 37 $\pm$ 0.5°C was 17.2 $\pm$ 0.5 mg/ml in FaSSGF and 0.068 $\pm$ 0.009 mg/ml in FeSSIF V2. The solubility sharply decreased with increasing pH as expected. This resulted in a low dipyridamole solubility of 0.017 $\pm$ 0.004 mg/ml in the final medium mixture at the end of the transfer experiment (FaSSGF : FeSSIF V2 = 1 : 2, pH 5.4), which was reasonably close to the value in pure FeSSIF V2.

Dynamic image analysis of the in-vitro drug precipitation transfer test

The dynamic image analysis revealed that following a lag time, the drug precipitated as complex particles. As shown in Figure 2, these particles were either star-like crystals or were formed through an instantaneous aggregation of elongated primary particles. Both flow rates of 4 and 9 ml/min led to the same habit of the forming particles. We confirmed this form of

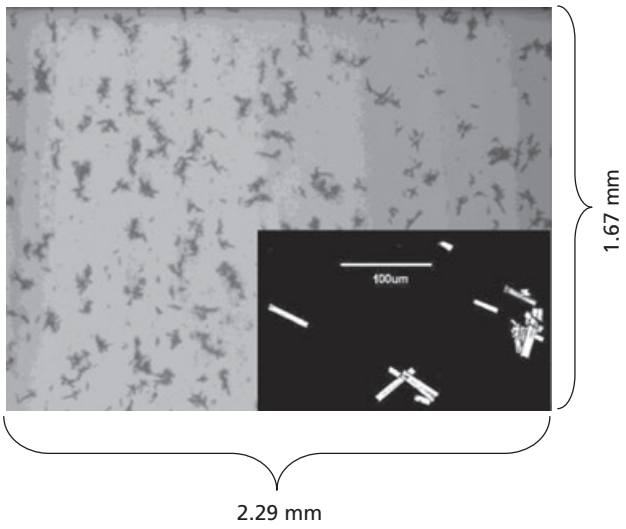

Figure 2 Dipyridamole precipitates in the acceptor phase at a flow rate of 9 ml/min after 3 h. Resulting picture of the XPT-C particle analyser, including an enlarged image captured with a microscope.

the particles/aggregates by directly taking samples for light microscopic analysis. Accordingly, the results were apparently not influenced by the pumping of medium into the camera system of the dynamic image analysis.

Figure 3a depicts the time-dependent sequence of the particle/aggregate concentration in the acceptor phase. For the high flow rate of 9 ml/min, a lag time of approximately 10 min and a maximum number of particles/aggregates was observed after 20 min. The lower transfer rate showed a longer lag time of approximately 20 min, which was explained by the slower increase in concentration in the acceptor phase compared with the higher transfer rate. A maximum particle/aggregate number was seen following approximately 30 min. The subsequent decrease in particle counts was probably the result of further particle aggregation and re-dissolution of a small particle fraction. Finally, after 1 h, the particle concentrations almost reached an equilibrium, showing no more differences between the flow rates.

Figure 3b and 3c show the particle/aggregate size distribution for different time points at a flow rate of 4 and 9 ml/min, respectively. Interestingly, not only the mean size, but also the width of the distribution changed over time. Thus, the peak of the size distributions shifted towards larger particle sizes over time. The obtained size distributions were comparatively broad and did not change between 60 and 180 min. Interestingly, the width of the particle aggregate distribution depended on the transfer rate.

In a next step, the results of the dynamic image analysis were compared with the concentrations of solubilised dipyridamole in the acceptor phase (Figure 4). The concentrations did not increase in a strictly cumulative manner. Decreasing values were observed once a marked crushing out of drug occurred. At the higher flow rate, the peak concentration was reached after 15 min, with a value of 0.65 ± 0.05 mg/ml. In contrast, at the lower flow rate of 4 ml/min, the maximum concentration of 0.47 ± 0.03 mg/ml was reached after 25 min.

Raman spectroscopy

Raman spectra were inline recorded as a function of time. Figure 5a shows the results of a selected wavelength range at the flow rate of 9 ml/min. The changes of the 1350 to 1400 cm^{-1} signal were of particular interest. Data recording started 40 min before the transfer test, returning only a small signal at the beginning of the experiment. The significant increase in the signal over the course of the transfer test correlated well with the amount of precipitated drug that was obtained from the HPLC data. Such change of Raman intensities over time was considered as an indicator for the onset of drug precipitation. At a flow rate of 9 ml/min, we observed the onset of nucleation after 13 min and at the flow rate of 4 ml/min, after 23 min.

To correlate the Raman intensities with the amounts of precipitated drug, we considered a broader range of the Raman spectrum from 504 to 2922 cm^{-1}. A partial least square model was found with four principal components, resulting in an R^2 value of 0.995 and the calibration line is depicted in Figure 5b using data at the transfer rate of 9 ml/min. The model showed that Raman monitoring was a sensitive tool for detecting drug precipitation in the acceptor vessel.

Mathematic modelling

It is generally known that precipitation is a two-step process composed of nucleation and particle growth.[10] For this reason our model assumptions started with established kinetic crystallisation equations.[16] At time $t = 0$ the solubilised amount of drug, M_{sol}, as well as the precipitated amount, M_{pr}, are 0. The parameter c_i is the effectively solubilised concentration of dipyridamole in the acceptor medium at time point t throughout the entire process and is described by:

$$c_i = \frac{M_{sol}}{V_i} \tag{3}$$

We divided the entire transfer and precipitation kinetics into four time intervals: (1) from the beginning to the start of nucleation (0, t_{nu}); (2) from the start of nucleation to the end of the medium transfer (t_{nu}, t_{tr}); (3) from the end of the medium transfer to the start of particle growth (t_{tr}, t_{gr}); and (4) from the beginning of particle growth to infinity (t_{gr}, ∞). The following equations apply to each time interval.

Interval 1 (0, t_{nu}):

$$\frac{dM_{sol}}{dt} = F_{tr} \cdot c_g \tag{4}$$

$$\frac{dM_{pr}}{dt} = 0 \tag{5}$$

$$V_i = V_{i0} + F_{tr} \cdot t \tag{6}$$

where F_{tr} describes the transfer rate used to pump FaSSGF, containing the solubilised drug, into FeSSIF. The parameter c_g represents the concentration of dissolved dipyridamole in FaSSGF (3 mg/ml).

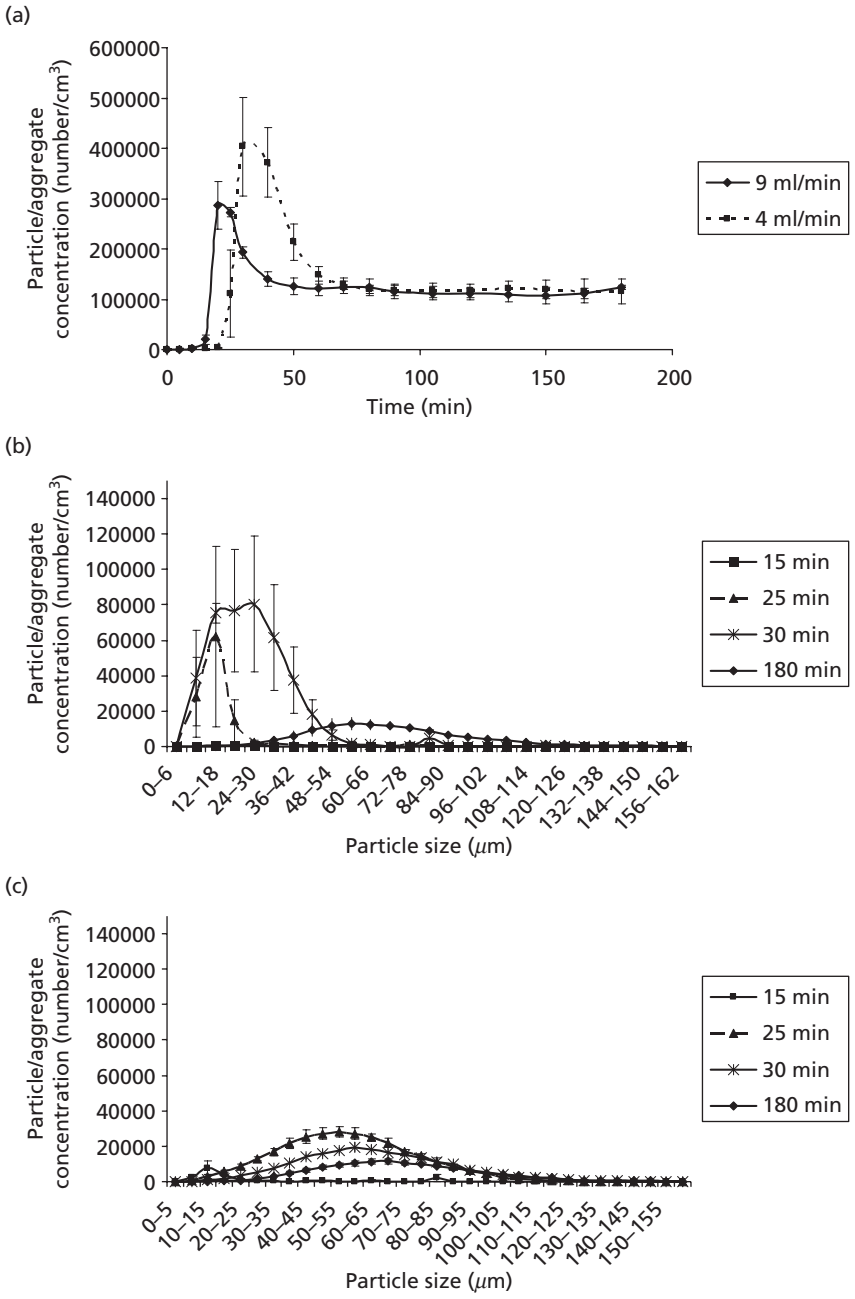

Figure 3 (a) Particle/aggregate concentrations of dipyridamole. (b) Size distribution at a flow rate of 4 ml/min. (c) Size distribution at a flow rate of 9 ml/min. Data are means ± SE.

Interval 2 (t_{nu}, t_{tr}):

$$\frac{dM_{sol}}{dt} = F_{tr} \cdot c_g - k_{nu} (c_i - c_{sat})^n \quad (7)$$

$$\frac{dM_{pr}}{dt} = k_{nu} (c_i - c_{sat})^n \quad (8)$$

$$V_i = V_{i0} + F_{tr} \cdot t \quad (6)$$

V_{i0} in the equation represents the initial volume of 500 ml at $t = 0$, while V_i stands for the volume at any time point t. The coefficient k_{nu} describes the nucleation constant, c_{sat} (0.017 mg/ml) the saturation concentration, and n represents the nucleation exponent.

Interval 3 (t_{tr}, t_{gr}):

$$\frac{dM_{sol}}{dt} = -k_{nu} (c_i - c_{sat})^n \quad (9)$$

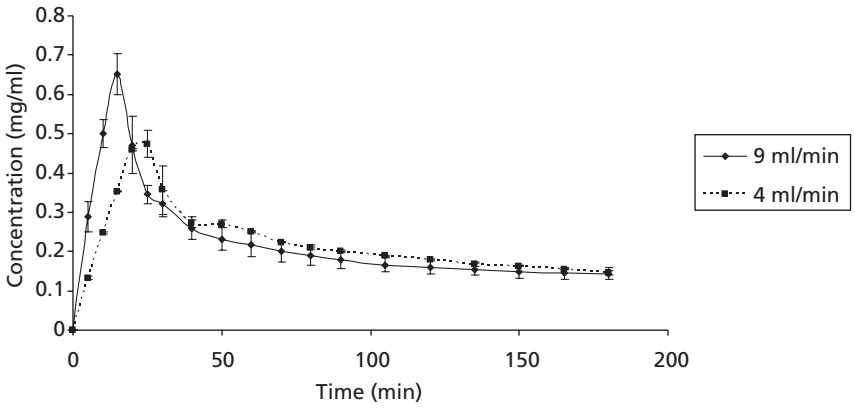

Figure 4 Profile of solubilised dipyridamole at a flow rate of 4 and 9 ml/min (means ± SE).

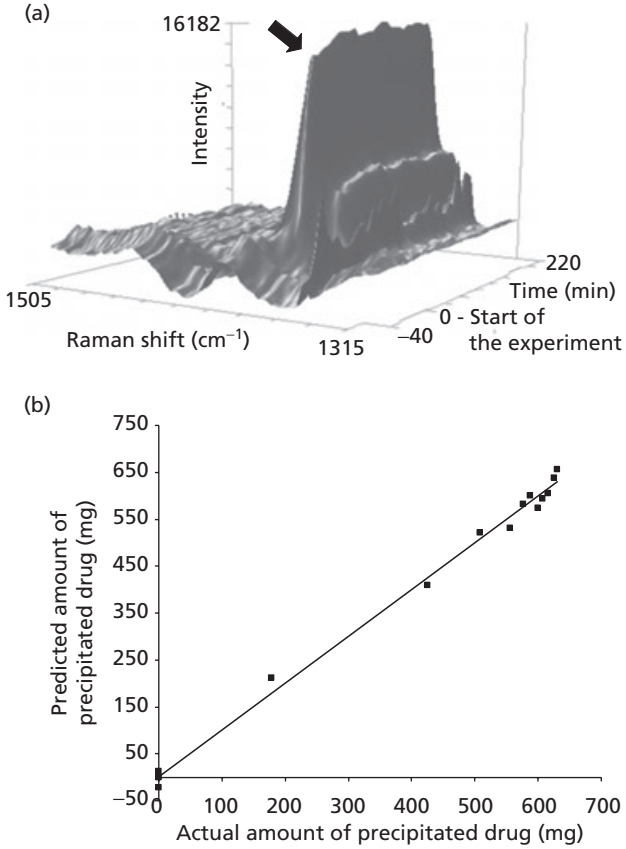

Figure 5 Results of the Raman measurements at a flow rate of 9 ml/min. (a) 3D plot of a Raman spectrum over the range 1315–1505 cm^{-1}. (b) Calibration line of the Raman partial least square model with the precipitated drug as response variable.

$$\frac{dM_{pr}}{dt} = k_{nu}(c_i - c_{sat})^n \quad (10)$$

$$V_i = V_{i0} + F_{tr} \cdot t_{tr} \quad (11)$$

Interval 4 (t_{gr}, ∞):

$$\frac{dM_{sol}}{dt} = -k_{gr}(c_i - c_{sat})^g \quad (12)$$

$$\frac{dM_{pr}}{dt} = k_{gr}(c_i - c_{sat})^g \quad (13)$$

$$V_i = V_{i0} + F_{tr} \cdot t_{tr} \quad (11)$$

where k_{gr} is the particle growth constant and *g* the corresponding particle growth exponent.

The above set of equations was fitted to the individual concentration profiles. Interestingly, the fits for the different flow rates revealed the same optimum with respect to their exponents. We found 5 for the nucleation exponent and 1.5 for the growth exponent. This consistent finding indicated that the different flow rates obviously produced the same type of drug precipitation process.

Examples of both flow rates are shown in Figure 6. There was excellent agreement between the model and the measured concentration profile over time. Interestingly, the profiles displayed a shoulder that followed the main peak. This shoulder marked the end of medium transfer into the simulated intestinal acceptor fluid. It was remarkable that the mathematical model was able to agree on this rather subtle effect of the concentration profile. The individual fitting curves resulted in parameter estimates that were averaged as displayed in Table 2.

Discussion

The in-vitro testing was performed using FaSSGF as acidic medium to simulate the gastric environment, whereas the acceptor medium was chosen not only based on the most updated biorelevant media composition but also for technical reasons. Thus, pure FeSSIF V2 showed the lower background signal in the XPT-C particle analyser compared with FaSSIF V2, making it better suited to study in-vitro drug precipitation. The combination of FaSSGF and FeSSIF V2 was therefore selected to study the change in pH *in vitro*, triggered by the transfer from the stomach to the intestine. The media selection had the advantage of a large pH change, however it was not

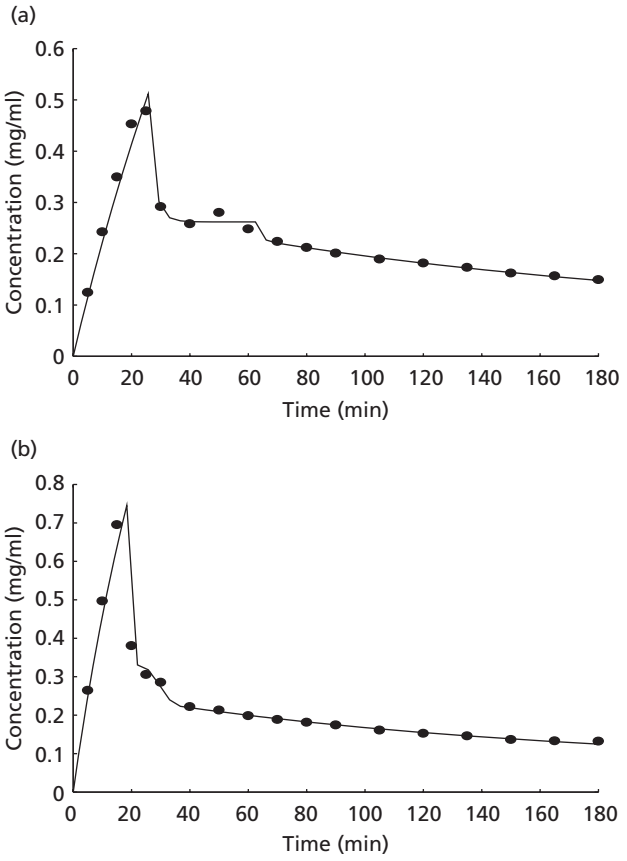

Figure 6 Examples of dipyridamole concentration profiles (points) together with the mathematical model (solid line) for a flow rate of 4 ml/min (a) and 9 ml/min (b).

Table 2 Estimated values of the fitted kinetic nucleation and growth model for the two transfer rates

	4 ml/min	9 ml/min
n	5	5
gr	1.5	1.5
k_{nu} (mean ± SE)	11 645.69 ± 385.53	6765.74 ± 2135.50
k_{gr} (mean ± SE)	7.47 ± 0.46	8.46 ± 0.29
t_{nu} (mean ± SE)	28.06 ± 0.88 min	18.52 ± 0.91 min
t_{gr} (mean ± SE)	68.01 ± 1.36 min	52.89 ± 17.96 min

gr, particle growth exponent; k_{gr}, particle growth constant; k_{nu}, nucleation constant; n, nucleation exponent; t_{gr}, start time of particle growth; t_{nu}, start time of nucleation.

possible to study an effect of the fasting versus fed state condition.

Another factor that needed consideration during the in-vitro test was the paddle speed. Previous experiments showed that this parameter had only a minor effect on the measured profiles in the acceptor phase.[5] For this reason an arbitrary constant paddle speed of 100 rev/min was selected for all experiments. The more important parameter for the in-vitro test was the transfer rate. It was not only relevant for the in-vitro results, but is also important for the in-vivo situation.[5] As the gastric emptying defines when a dissolved drug in the stomach is transferred to the intestinal fluid, we used different flow rates *in vitro* that were considered to be relevant for physiological gastric emptying.[5]

Using dynamic image analysis it was demonstrated that the transfer rate was affecting the precipitation kinetics. A common aspect of the investigated transfer rates was that similar complex particles/aggregates were obtained. The mean particle size and size distribution as well as the concentration profile showed a clear dependence on the transfer rate. Based on particle number and size, the dynamic image analysis agreed with the observed decreasing drug concentration due to precipitation in both cases. However, care is needed when comparing the size and concentration data on a quantitative basis, since the density of the particles/aggregates is unlikely to stay constant over time. For this reason we did not include the dynamic image analysis data for modelling of the concentration profiles.

The faster transfer rate provided the higher drug concentration peak in the intestinal medium. It could therefore be hypothesised that under such conditions the absorption process is also promoted *in vivo*. However, our transfer test did not consider any drug absorption. Unlike the situation *in vivo*, no permeation step was involved *in vitro* so that no continuous removal of drug from the bulk solution could be taken into account. More research is therefore needed to clarify the biorelevance of the current in-vitro transfer test.

However, at the level of the in-vitro test itself, the new monitoring tools provided insights into the process of in-vitro drug precipitation. Disperse Raman spectroscopy was found to be particularly useful. It enabled the onset of precipitation to be defined and the amount of precipitated drug to be followed. The latter was in good agreement with the concentration data gathered by HPLC analysis. Raman spectroscopy appears to be a valuable tool for the monitoring of biopharmaceutical tests, as recently highlighted by Savolainen *et al*.[19] That work studied the in-situ solid state of indometacin and carbamazepin in a flow-through dissolution test. The authors were able to follow changes from the amorphous drug to the crystalline state during the dissolution process. Such changes in the solid state properties can be of biopharmaceutical relevance and possibly depend on the dissolution medium used. In particular the biorelevant media can influence a solvent-mediated solid phase transformation.[20]

For the transfer test it was of interest to see if the drug undergoes changes in solid state structure during the precipitation process. Even though a drug can potentially precipitate in an amorphous form or as a hydrate, the Raman spectrum of the precipitated model compound dipyridamole revealed no differences compared with its initial crystalline form.

In addition to gaining a better understanding of in-vitro drug precipitation kinetics by using analytical monitoring tools, mathematical modelling also provided valuable insights. We used power laws to model nucleation as well as the growth of the particles. Based on minimum root mean square error values, the best models had the same exponents for both transfer rates. The nucleation exponent of 5 delivered by the model was well within the expected range of 3–6.[16] It should be emphasised that the formation of drug nuclei and the concentration differences in solution showed a highly

non-linear relationship. The particle growth exponent returned by the model was 1.5. It is interesting to note that this growth exponent was found to be greater than 1. A simple approximation for particle growth would be a first order inverse dissolution process according to Noyes Whitney, resulting in a particle growth exponent of 1. This type of particle growth was previously applied by Sugano.[15] However, exponents greater than 1, as observed in our experiments, were also in line with previous experimental findings.[16] They probably originate from geometric effects, as complex structures of particles and surfaces can be the result of a precipitation/aggregation process,[21] resulting in deviation from a simple first order model.[22,23] Accordingly, our growth exponent of 1.5 rather than 1 may be the result of a complex particle surface, which defines the true surface area being available for drug dissolution and/or precipitation. This assumption of a complex surface agreed well with the images obtained from online monitoring, which demonstrated the complex geometry of the precipitated particles/aggregates. It would be interesting to determine from future tests how the exponents depend on surface properties of precipitated drugs other than dipyridamole.

The mathematical model was also of particular interest in the determination of nucleation onset. This time point is difficult to assess by experimental means since the initial nuclei are expected to be subvisible as well as unstable. Accordingly, the image analysis can only detect particles over a size range of a few micrometers and also Raman spectroscopy has a limited resolution with respect to detecting a small fraction of crystalline drug. Given these limitations, it is remarkable that the calculated nucleation time (Table 2) agreed well with the precipitation onset determined by Raman spectroscopy as well as obtained from dynamic image analysis.

Inline Raman spectroscopy and online dynamic image analysis, as well as HPLC data provided a coherent view of the precipitation process. The in-vitro tools allowed suitable monitoring of the process and the mathematic model facilitated an improved understanding of the in-vitro drug precipitation. The obtained model coefficients are expected to be specific for a pharmaceutical compound in a given medium. Determination of these coefficients is of special interest with respect to mechanistic drug absorption modelling. These parameters can be used as input data for physiologically based pharmacokinetic models. Such mechanistic modelling is today available from a few commercial software packages. However, the mathematical models presently do not consider the precipitation process in its full complexity, that is through consideration of a separate nucleation and growth step. Consequently, the physiologically based pharmacokinetic models need to be refined in that respect and our calculated coefficients could then serve as input parameters to obtain mechanistically improved simulations for drug absorption.

Conclusions

Using a biorelevant transfer test, we examined precipitation of dipyridamole *in vitro*. Novel analytical methods were introduced together with a mathematical model for nucleation and particle growth. The dynamic image analysis revealed a complex structure of the precipitated particles/aggregates, which was also reflected in the mathematical model by a growth exponent differing from 1. The particle size distribution changed as a function of time and differences between the transfer rates were mainly observed in the initial phase of the precipitation. These observations also agreed with the findings of the inline Raman spectroscopy, which was demonstrated to be an excellent tool for monitoring the precipitated drug fraction.

It can be concluded that a simple measurement of drug concentration in the acceptor phase does not provide a complete characterisation of in-vitro drug precipitation. The underlying processes are highly complex, especially in biorelevant media, and so further analytical tools are required. The combined efforts of modelling and advanced analytical monitoring provide important insights into drug nucleation and particle growth. Furthermore, the results can be used for subsequent mechanistic absorption modelling. Physiologically based absorption modelling can facilitate correlations with in-vivo findings. Accordingly, we must have a good understanding of the in-vitro results to enable meaningful in-vivo correlations. This is also the key to better optimising the in-vivo performance of pharmaceutical formulations based on in-vitro results.

Declarations

Conflict of interest

The Author(s) declare(s) that they have no conflicts of interest to disclose.

Funding

This research received no specific grant from any funding agency in the public, commercial or not-for-profit sectors.

Acknowledgements

Support with Raman measurements from Dr Carsten Uerpmann (Kaiser Optical Systems, USA) is gratefully acknowledged.

References

1. Badawy SIF *et al*. Formulation of solid dosage forms to overcome gastric pH interaction of the factor Xa inhibitor, BMS-561389. *Pharm Res* 2006; 23: 989–996.
2. Blum RA *et al*. Increased gastric pH and the bioavailability of fluconazole and ketoconazole. *Ann Int Med* 1991; 114: 755–757.
3. Charman WN *et al*. Physicochemical and physiological mechanisms for the effects of food on drug absorption: the role of lipids and pH. *J Pharm Sci* 1997; 86: 269–282.
4. Russell TL *et al*. pH-related changes in the absorption of dipyridamole in the elderly. *Pharm Res* 1994; 11: 136–143.
5. Kostewicz ES *et al*. Predicting the precipitation of poorly soluble weak bases upon entry in the small intestine. *J Pharm Pharmacol* 2004; 56: 43–51.
6. Zhou R *et al*. pH-dependent dissolution in vitro and absorption in vivo of weakly basic drugs: development of a canine model. *Pharm Res* 2005; 22: 188–192.
7. Sugawara M *et al*. The use of an in vitro dissolution and absorption system to evaluate oral absorption of two weak bases in pH-independent controlled-release formulations. *Eur J Pharm Sci* 2005; 26: 1–8.

8. Gu C *et al*. Using a novel multicompartment dissolution system to predict the effect of gastric pH on the oral absorption of weak bases with poor intrinsic solubility. *J Pharm Sci* 2004; 94: 199–208.
9. Jantratid E *et al*. Dissolution media simulating conditions in the proximal human gastrointestinal tract: an update. *Pharm Res* 2008; 25: 1663–1676.
10. Kirwan DJ, Orella CJ. Crystallisation in the pharmaceutical and bioprocessing industries. In: Myerson AS, ed. *Handbook of Industrial Crystallization*, 2nd edn. Woburn, MA: Butterworth-Heinemann, 2002.
11. Lindfors L *et al*. Nucleation and crystal growth in supersaturated solutions of a model drug. *J Colloid Interface Sci* 2008; 325: 404–413.
12. Shekunov BY, York P. Crystallization processes in pharmaceutical technology and drug delivery design. *J Cryst Growth* 2000; 211: 122–136.
13. Lamer V, Dinegar R. Theory, production and mechanism of formation of monodispersed hydrosols. *J Am Chem Soc* 1950; 72: 4847–4854.
14. Brouwers J *et al*. Supersaturating drug delivery systems: the answer to solubility-limited oral bioavailability? *J Pharm Sci* 2009; 98: 2549–2572.
15. Sugano K. A simulation of oral absorption using classical nucleation theory. *Int J Pharm* 2009; 378: 142–145.
16. Vauck WRA, Müller HA. *Grundoperationen Chemischer Verfahrenstechnik*, 10th edn. Leipzig/Stuttgart: Deutscher Verlag für Grundstoffindustrie, 1994.
17. Thieme RÖMPP Online, Stuttgart, Georg Thieme KG, 2010. http://www.roempp.com/prod/
18. Lunn G, Schmuff NR. *HPLC Methods for Pharmaceutical Analysis*, 1st edn. New York: Wiley, 1997.
19. Savolainen M *et al*. Better understanding of dissolution behaviour of amorphous drugs by in situ solid-state analysis by means of Raman spectroscopy. *Eur J Pharm Biopharm* 2009; 71: 71–79.
20. Letho P *et al*. Solvent-mediated solid phase transformations of carbamazepine: effects of simulated intestinal fluid and fasted state simulated intestinal fluid. *J Pharm Sci* 2009; 98: 985–996.
21. Lin MY *et al*. Universality in colloid aggregation. *Nature* 1989; 325: 360–362.
22. Valsami G, Macheras P. Determination of fractal reaction dimension in dissolution studies. *Eur J Pharm Sci* 1995; 3: 163–169.
23. Macheras P, Iliadis A. *Modeling in Biopharmaceutics, Pharmacokinetics, and Pharmacodynamics*, 1st edn. New York: Springer, 2002.